# Electron Energy Distribution Function Measurements by Langmuir Probe in ITER like Negative Ion Sources

B. Crowley, D. Homfray, U. Fantz, D. Boilson, and R. S. Hemsworth

Citation: AIP Conf. Proc. **925**, 193 (2007); doi: 10.1063/1.2773660
View online: http://dx.doi.org/10.1063/1.2773660
View Table of Contents: http://proceedings.aip.org/dbt/dbt.jsp?KEY=APCPCS&Volume=925&Issue=1
Published by the American Institute of Physics.

# Electron Energy Distribution Function Measurements by Langmuir Probe in ITER like Negative Ion Sources

[1]B. Crowley, [1]D. Homfray, [2]U. Fantz, [3]D. Boilson and [4]R.S. Hemsworth

*1. Euratom/UKAEA Fusion Association, Culham Science Centre, Abingdon, Oxon. OX14 3DB, UK.*
*2. Association Euratom-IPP, IPP Garching, Germany*
*3. Association Euratom/DCU Plasma Research Laboratory, Dublin City University, Dublin 9, Ireland*
*4. Association Euratom-CEA, CEA Cadarache, F-13108, St. Paul lez Durance, France*

**Abstract.** Determining $d^2I/dV^2$ from a traditional Langmuir probe trace using numerical techniques is inherently noisy and generally yields poor results. We have developed a Langmuir probe system based on a method first used in the 1950's by Boyd and Twiddy [1]. The system measures the 2nd derivative directly. This paper presents results from the driver and extraction regions of the KAMABOKO III ITER like negative ion source.

## INTRODUCTION

The development of a high yield $H^-$ (or $D^-$) ion source capable of long pulse operation is an essential step towards the realisation of a neutral beam heating system for ITER. Development on two possible candidate ion sources is presently being carried out. In Cadarache, France, the KAMABOKO III ion source (Fig.1)(i.e. a caesiated, filamented, multi-pole arc discharge source) is being studied and in Garching, Germany inductively coupled RF sources are being studied. These systems are fully described elsewhere [2,3]. Optimising these sources requires a delicate balance in the $H^-$ production and destruction processes. A key feature of both ion sources is the separation of the driver region from the extraction region by means of the magnetic filter field. The filter field keeps the electron temperature at the extraction grid low in order to minimise the destruction of $H^-$ ions through the process of electron detachment ($e+H^- \rightarrow e+H+e$). The cross section for this process increases by 3 orders of magnitude over the electron energy range from 1 to 10 eV. Hence for optimisation of the source it is important to know the electron temperature. To this end Langmuir probes are used to measure the plasma parameters ($T_e$, $n_e$ and $V_p$) in front of the extraction grid and in the driver region. However, the electron energy distribution function (EEDF) in low pressure plasmas is generally non-Maxwellian even at the low electron energy range and application of conventional theory can lead to significant errors. In non-Maxwellian plasmas, the electron temperature can be thought of as an effective electron temperature corresponding to a mean electron energy determined from the integrals of the EEDF.

CP925, *Production and Neutralization of Negative Ions and Beams, 11th International Symposium,* edited by M. P. Stockli

## BACKGROUND

Langmuir probes are vital diagnostic tools in the study of low pressure weakly ionised plasmas. Local measurements of various plasma parameters are possible using Langmuir probes making them superior to many other diagnostic techniques. These strongly non-equilibrium plasmas are characterised by an electron temperature that is much higher than the ion or neutral gas temperature. Moreover the EEDF itself is generally non-Maxwellian, particularly in arc driven systems where the plasma is sustained by primary electrons falling through a potential of approximately 100 volts.

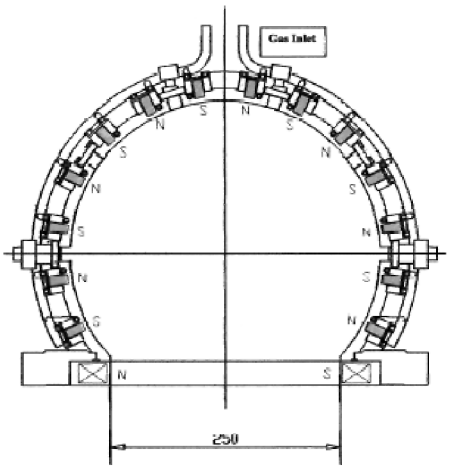


**FIGURE 1.** Cross Section of KAMABOKO III Ion Source.

Many probe theories [4,5,6,7] have been developed over the years to determine the plasma parameters from probe traces under various conditions. These theories apply to either ion collection by a probe or electron collection however most theories assume the plasma has an isotropic Maxwellian electron distribution. Analysis of non-Maxwellian plasmas using these techniques yields misleading results [8].

The Druyvesteyn [9]. extension of the Langmuir and Mott-Smith probe theory [7] allows the determination of the electron energy spectrum. Druyvesteyn shows that the EEDF may be found from the expression,

$$N(\in) = \frac{2}{Ae^2}\left(\frac{2m \in}{e}\right)^{\frac{1}{2}} \frac{d^2 I}{dV^2} \qquad (1)$$

where $N(\in)d\in$ is the number of electrons per unit volume with energy in the interval $[\in\ ,\ \in+d\in]$ eV, $V$ is the probe voltage, $\in$ is the probe voltage with respect to the

plasma potential $V_p$, ($\in = V_p - V$), $A$ is the probe area, $d^2I/dV^2$ is the second derivative of the current-voltage characteristic and $e$ and $m$ are the electronic charge and mass.

The electron density, $n_e$, is obtained from the integral of $N(\in)$.

$$n_e = \int_0^\infty N(\in) d \in \tag{2}$$

In the case of a non-Maxwellian electron energy distribution the electron temperature can be thought of as an effective electron temperature defined as,

$$T_{eff} = \frac{2}{3}\langle \in \rangle = \frac{2}{3n_e}\int_0^\infty \in N(\in) d \in \tag{3}$$

However determining $d^2I/dV^2$ from a traditional Langmuir probe trace using numerical techniques is inherently noisy and generally yields poor results.

An alternative method first used in the 1950's by Boyd and Twiddy [1] is to superimpose a modulated ac voltage ($e_m$) on the probe voltage $V$; the superimposed voltage can be represented as

$$e_m = E\left[\frac{1}{2} + \frac{2}{\pi}(\cos pt - \frac{1}{3}\cos 3pt + ...., etc)\right]\cos \omega t \tag{4}$$

,

Where E is the peak of the modulated signal, and $p$ and $\omega$ are the frequencies of the modulation and carrier signals respectively.

By Taylor's Theorem the probe current can be expressed as,

$$I = f(V + e_m) = f(V) + e_m f'(V) + \frac{e_m^{\ 2}}{2!} f''(V)..... \tag{5}$$

The component of current measured at frequency $p$ receives contributions only from even-order derivatives, provided that $\omega$ is not an even multiple of $p$, and is given by,

$$i_p = \left[\frac{E^2}{2!}\frac{1}{\pi} f''(V) + \frac{E^4}{4!}\frac{3}{8}\left(\frac{1}{4} + \frac{1}{\pi^2}\right) f''''(V) + .....etc\right]\cos pt \tag{6}$$

Terms involving the fourth and higher order derivatives can be neglected, hence the second derivative may be obtained from a direct measurement of $i_p$. In practical units the EEDF is given by.

$$N(\in) = \frac{8\pi}{A}\left(\frac{m \in}{e^3}\right)^{\frac{1}{2}} \frac{i_p(rms)}{E^2} \mathbf{(eV)^{-1}\,cm^{-3}} \tag{7}$$

The effect of the finite value of the ac amplitude on the measurement of the 2nd derivative as reported in [10] was minimised by varying the value of $E$ from 0.1V just below the expected plasma potential where the 2nd derivative is high to 1 V in the ion collection region where the 2nd derivative is small. This variation was done in an exponential fashion in order to optimise simultaneously the signal to noise ratio and the energy resolution. The system was found to reproduce faithfully (to within 1%) the expected 2nd derivative of various non-linear current-voltage characteristics obtained from passive circuits [11].

## Caveat

The validity of the Druyvesteyn formula (equation 1) is limited by the condition $\lambda_e >> r_s$ where $r_s$ is the radius of the sheath around the probe and $\lambda_e$ is the electron mean free path. In the case of probe operating in a magnetic field the limiting condition is $\rho_e >> r_s$ where $\rho_e$ is the Larmor radius of the electron [12,13]. The results presented in this paper all pertain to low pressure scenarios (~.3 Pa) where the condition $\lambda_e >> r_s$ holds true and the condition $\rho_e >> r_s$ holds true for all data except data points measured close to chamber wall (the first point in Fig. 7). In cases where these conditions are not met electron depletion will cause distortions of the second derivative of the probe characteristic, hence the actual measurement is not $d^2I/dV^2$ but rather the measurement is a convolution of $d^2I/dV^2$ and the instrumental function of the differentiating method $\phi(V-V')$ i.e. what is measured is:

$$\frac{d^2J}{dV^2} = \int \frac{d^2I}{dV'^2}\phi(V-V')dV' \tag{8}$$

To correctly obtain the EEDF a deconvolution procedure must be applied and knowledge of $\phi(V-V')$ is required.

# EXPERIMENTAL SET-UP

## Hardware

The tungsten probe is mounted on a ceramic shaft that is housed in a bellows type motorised linear drive mechanism. This allows precise positioning of the probe for spatial scans across the chamber along the mid plane at a distance of 17 mm in front of plasma grid.

A schematic of the experimental set-up is shown in Fig. 2. The controlling PC contains a National Instruments M-series data acquisition card. The card is a 16 bit 2.5 Msamples $s^{-1}$ with 4 analogue output and 16 analogue input channels. Output channels from the card are connected to a KEPCO bipolar operational power supply. The power

supply has a voltage range of ±100 V, a current rating of 1 Amp and 20 kHz bandwidth. The output of the power supply is connected to the probe and the current drawn on the probe fed to a 2 channel isolation amplifier. The signal at one channel has its dc component removed before amplification via a suitable gain resistor to a –10 to 10 V signal which is returned to the data acquisition card for analysis. The other signal is ac filtered, amplified and returned to the data acquisition card. The PC and all the electronics are powered from the mains through an isolation transformer and the common ground for all the equipment is the source wall.

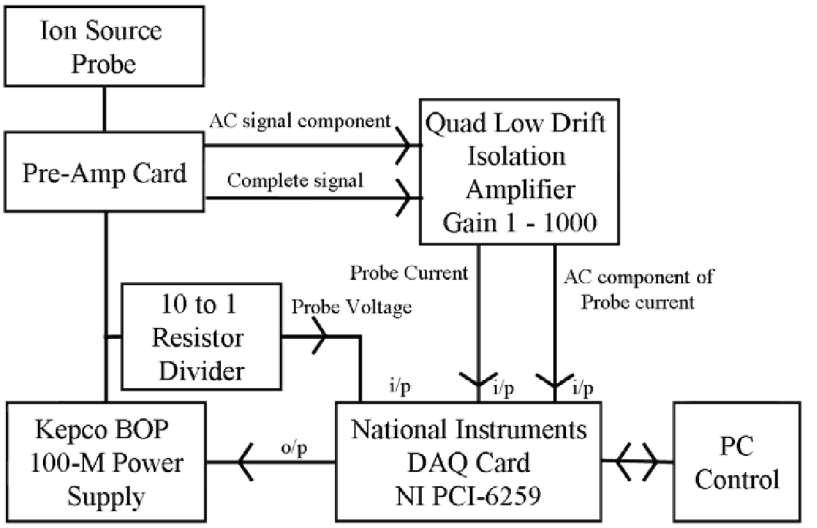


**FIGURE 2.** Schematic of Experimental Set-up.

## Software

A LabVIEW™ computer program was developed to run the data acquisition and the data analysis. The program generates the output waveform to the Kepco power supply. The output waveform consists of a dc bias with the modulated ac signal ($e_m$) superimposed. The frequency settings used throughout were $\omega$=10 kHz and $p$= $\omega/5$, the dc bias was swept from –20 to 20 V and $E$ was varied from .01 to 1 V.

The program reads the probe current signals and performs fast Fourier transform on the ac component of the current and records the phase and amplitude of both the carrier and modulation frequency component dc probe voltage. The dc value of the probe current is also recorded in order to generate a traditional Langmuir probe trace for alternative analysis.

## ANALYSIS

The plasma potential is found from the zero of the 2nd derivative i.e. the voltage at which there is a 180º phase change in the Fourier transform coefficient of the

modulation frequency. The EEDF is then determined and the integrals evaluated to obtain the electron density and the effective electron temperature. The EEDF data is fitted to the Druyvesteyn formula, $N(\in) = a \in^{0.5} \exp(b \in^{c})$, using a non-linear least squares fitting method.

The traditional Langmuir probe *I-V* characteristic trace is analysed using the following methods.

i. The Orbital Motion Limited (OML) theory of ion collection [5,7].
ii. The Allen-Boyd-Reynolds (ABR) radial motion theory of ion collection [4].
iii. Bernstein-Rabinowitz-Laframboise (BRL) theory of ion collection [6].
iv. Classical Langmuir-Mott Smith (LMS) theory for electron collection [7].

In all cases the pertinent data is extracted from the trace and is fitted to the theory using the Levenberg-Marquart non-linear fitting method. Classical Langmuir theory determines an electron temperature based on the assumption that the electrons have a Maxwellian distribution. OML, BRL and ABR theories can be used to infer electron temperature but these methods are very unreliable as only a small portion of the electrons in the high energy range are considered. The energy distribution in this range is very likely to differ from the rest of the distribution unless there is a strong influence of electron-electron interactions. Hence it is preferable to use Langmuir theory to infer $T_e$ and then use this value to fit the OML, BRL and ABR theories.

# RESULTS

## Comparison of Boyd-Twiddy Method with Traditional Method

Figures 3 to 6 show the data obtained for a typical shot. In this case the cylindrical probe was positioned near the centre of the discharge in the extraction region, the arc power was 47 kW and the gas pressure was 0.3 Pa. The results are summarised in table 1. Figure 3 shows the Langmuir probe IV curve raw data (open circles); this data

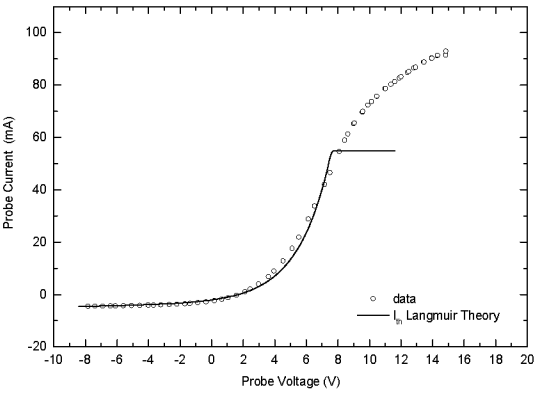


**FIGURE 3**. Langmuir probe trace raw data and electron current best fit.

**TABLE** 1. Summary of results from IV curve shown in Fig. 3

| $V_p$ V | $V_f$ V | $T_e$ (LMS) eV | $T_{eff}$ (BT) eV | $n_e$ (BT) $cm^{-3}$ | $n_e$ (LMS) $cm^{-3}$ | $n_e$ (OML) $cm^{-3}$ | $n_e$ (ABR) $cm^{-3}$ | $n_e$ (BRL) $cm^{-3}$ |
|---|---|---|---|---|---|---|---|---|
| 7.6 | 1.56 | 2.05 | 2.98 | $1.6\times10^{12}$ | $9\times10^{11}$ | $1.5\times10^{12}$ | $5.5\times10^{11}$ | $1.7\times10^{12}$ |

is fitted to the classical Langmuir theory (solid line) applied to the electron retardation region when the probe potential is less than the plasma potential. The theory assumes a Maxwellian electron distribution but it is clear from the figure that the theory does not fit the data very well between 2 and 6 volts. The 2nd derivative of the IV curve from Fig. 3 is presented in Fig. 4. The figure also shows the 2nd derivative as obtained by both a standard numerical method (···Δ···) and the Boyd-Twiddy method (—●—). Obtaining the result by a numerical method requires smoothing of the data between successive differentiation operations and the outcome is subject to the choice of smoothing method employed [14]. The Boyd-Twiddy method on the other hand does not require any subjective analysis and it results in a smoother curve than the former method.

The plasma potential is found to be 7.6 ±0.5 Volts and the floating potential is found from the zero of the Langmuir probe trace to be 1.56 Volts. The error in the measured value of the plasma potential can translate to an error of up to 20% in the parameters derived using this value. The data from the 2nd derivative (Boyd-Twiddy method) is used to evaluate the EEDF. This EEDF is shown in Fig. 5 where it is fitted to the Druyvesteyn formula, $N(\in) = a \in^{0.5} \exp(b \in^{c})$, for two values of parameter $c$ *i.e* $c$=1 for a Maxwellian distribution and for a least squares best fit value for $c$ in the

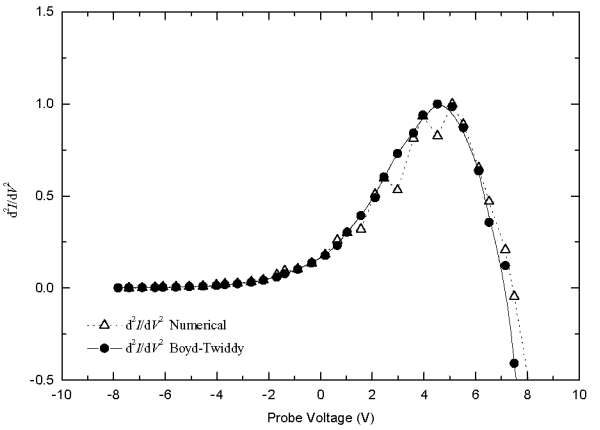


**FIGURE 4.** 2nd derivative of the IV curve showing numerical and BT method. Measurement acquired with a cylindrical probe at the centre of the discharge with arc power is 47 kW and the gas pressure 0.3 Pa.

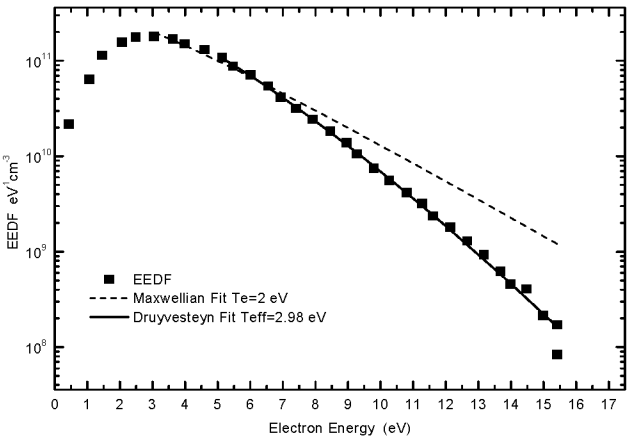


**FIGURE 5.** Plot of EEDF acquired with a cylindrical probe and fitted Maxwellian and Druyvesteyn distributions. Measurement taken at the centre of the discharge with arc power is 47 kW and the gas pressure 0.3 Pa.

Druyvesteyn formula. It is clear that a Maxwellian is not the best fit for the data. Integrating the data from Fig. 5 according to equations 3 and 4 gives $n_e$=1.6×10$^{12}$ cm$^{-3}$ and $T_{eff}$=2.98 eV. Analysis of the electron retardation region of the *I-V* curve using classical Langmuir theory yields $n_e$=9×10$^{11}$ cm$^{-3}$ and $T_e$=2.05 eV. An increase from 2 eV to 3 eV in the electron temperature results in a change from 1×10$^{-17}$ cm$^2$ to 1.1×10$^{-16}$ cm$^2$ in the value of the cross section for electron impact detachment of $H^-$ [15].

Figure 6 shows the ionic current fitted to the different theories of ion collection. It was found that the BRL theory fits the data better than the others. This is not surprising since the BRL theory is the most complete (and most difficult to implement), taking account of sheath expansion, collisions and finite ion temperature. The BRL theory is fitted to the data following a procedure described in [16].

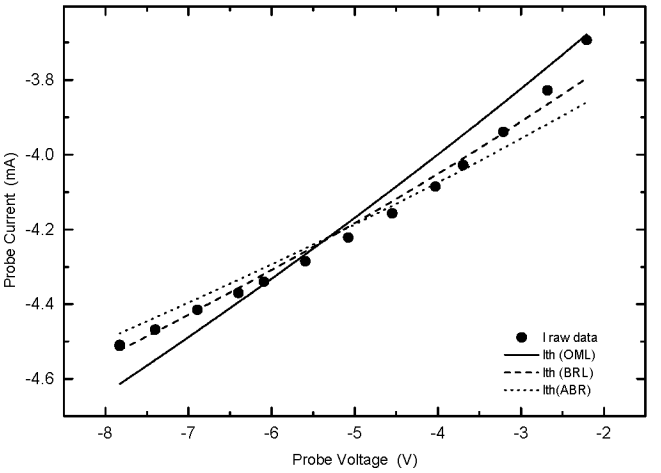


**FIGURE 6.** The ion current fitted to ABR OML and BRL theories of ion collection. The data was acquired with a cylindrical probe. The source conditions were 47 kW 0.3 Pa.

## Plasma Parameters in the Extraction Region of the Kamaboko III Ion Source

The plasma parameters were measured using the cylindrical probe as a function of arc power, source pressure, and as a function of probe position. A summary of the results are presented in Figs. 7 to 9. In each figure $T_e$ and $T_{eff}$ are presented on the bottom graph and the plasma density is presented on the top graph.

Figure 7 shows the plasma parameters as a function of position from the wall to the centre of the source. The axis is parallel to the extraction plane and the axial position is 17 mm from the plasma grid, parallel to the direction of magnetic filter field. For the scan the arc power was kept at a constant 47 kW and the source pressure was 0.3 Pa. The first point in the scan is taken in the magnetic field cusp so the probe data for this point is unreliable. It is found that the electron temperature decreases towards the centre of the source and that $T_{eff}$ is consistently about 1eV greater than $T_e$. The plasma density decreases significantly towards the centre of the source. This non-uniform plasma density across the source makes it difficult to extract a uniform large area beam from the source.

Figure 8 shows the results of a pressure scan. The power was 47 kW and the results presented are for the central position. The density is maximum at 0.3 Pa and the electron temperature decreases with increasing pressure.

The results of the power scan measured in the centre of the discharge with source pressure of 0.3 Pa is shown in Fig. 9. The figure shows that the density increases strongly (from $5\times10^{11}$ to $1.5\times10^{12}$ $cm^{-3}$) over a power range 25-65 kW, whilst the electron temperature increase only slightly (< 1 eV) across the same power range.

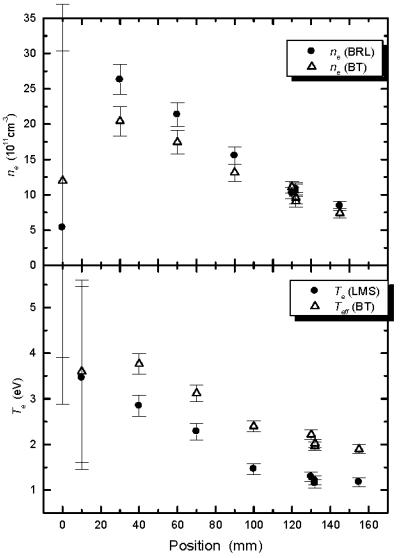


**FIGURE 7.** Plasma parameters as a function of position from the edge to the centre of the source. The data was acquired with a cylindrical probe. The arc power was 47 kW and the pressure was 0.3 Pa.

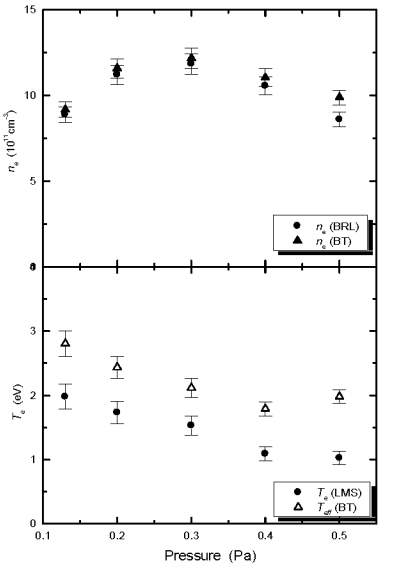


**FIGURE 8.** Plasma parameters measured at the centre of the discharge as a function of Pressure. The data was acquired with a cylindrical probe. The arc power was 47 kW.

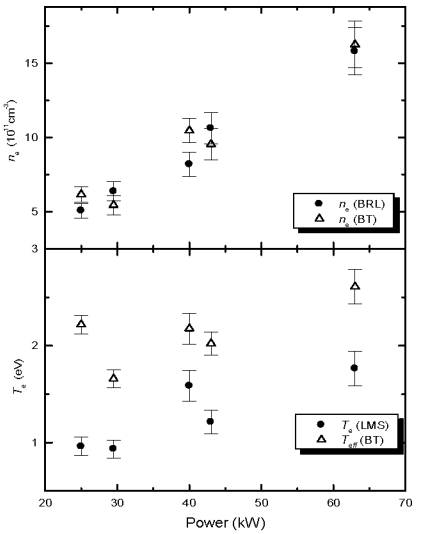


**FIGURE 9.** Plasma parameters in the centre of the discharge as a function of arc Power. The data was acquired with a cylindrical probe. The pressure was 0.3 Pa.

## Plasma Parameters in the Driver Region of the Kamaboko III Ion Source

The measurements made in the driver region of the source were limited, at this time for practical reasons, to low power operation (20 kW). The evolution of the form of the EEDF over a range of pressure is shown in Fig. 10. It can be seen that form of the

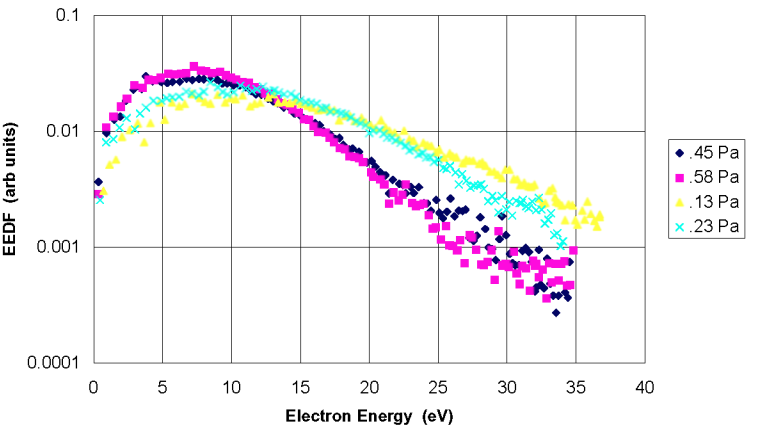


**FIGURE 10.** EEDF plotted for four different gas pressures; data taken at 20 kW in the Driver region.

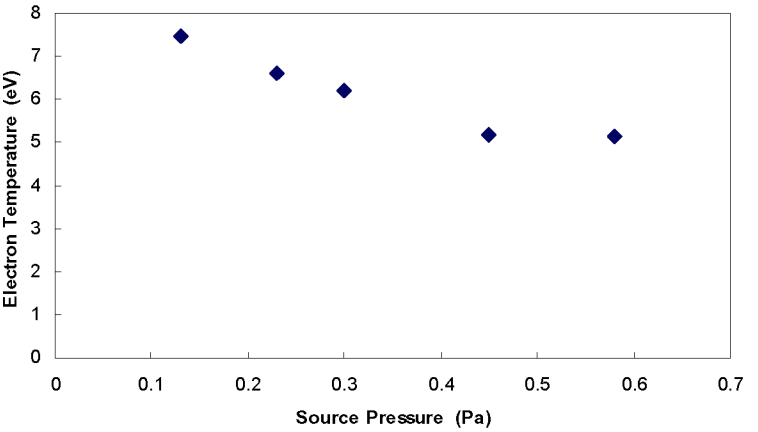


**FIGURE 11.** Electron Temperature in the centre of the driver region as a function of Source pressure. The data were acquired with a cylindrical probe and the arc power was 20 kW.

EEDF is basically a single temperature distribution at this low power. However one shot at higher power (before the probe disintegrated) showed that the form had evolved into a two temperature distribution. Electron temperature and electron density as a function of pressure are shown in Figs. 11 and 12. The electron temperature is found to decrease from 7.5 eV to 5 eV with increasing pressure. at a pressure of 0.3 Pa the electron temperature is 6.4 eV in the driver region compare to 2.2 eV in the extraction region for similar power. The density peaks at about 0.3 Pa this is the same pressure at which the peak occurs in the extraction region but the peak value in the

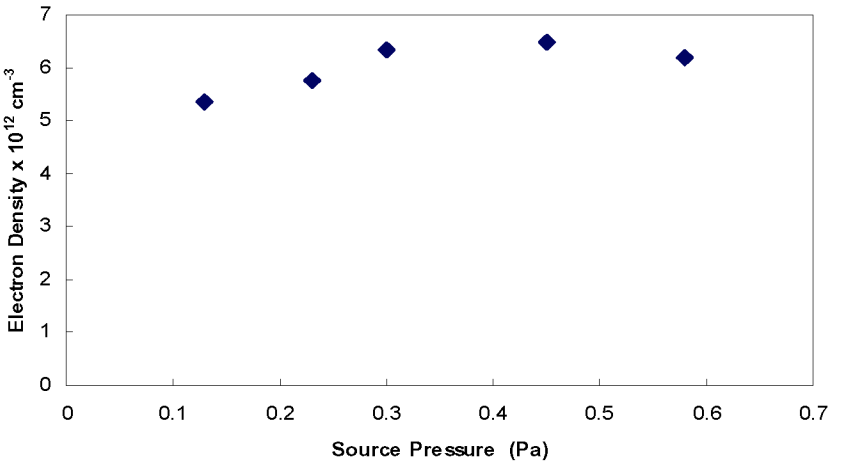


**FIGURE 12.** Electron Density in the centre of the driver region as a function of Source pressure. The data was acquired with a cylindrical probe and the arc power was 20 kW.

driver is about an order of magnitude higher. The density peak can be explained by the fact that as the pressure increases there is more gas to ionise so the density firstly increases. However the increased pressure also causes the electron temperature to decrease due to the increase in electron neutral collisions. This decreased temperature in turn reduces the ionisation rate so less ions are produced and the density decreases.

## The EEDF and Optical Emission Spectroscopy

Optical emission spectroscopy (OES) is a powerful diagnostic tool and is employed routinely in the field of negative ion source development. Provided an absolute calibration of the OES system is available, a variety of plasma and gas parameters can be determined. This includes molecular hydrogen density, atomic hydrogen density and negative ion density. Full details of the capability of the OES system in relation to ion source development is available in reference [3]. In general terms the parameter in question is related to the absolutely calibrated line emission via a collisional radiative (CR) model.

$\varepsilon_{pk} = n\ n_e X_{pk,eff}(T_e, n_e, ...)$ where,

$\varepsilon_{pk}$ is the line emission, $n$ is the species density, $X_{pk,eff}(T_e, n_e, ...)$ represents an effective emission rate coefficient. However this rate coefficient derived from the CR model can be sensitive to the form of EEDF. Hence knowing the form of the EEDF can help refine these models.

Figure 13 shows 3 fits to normalised EEDFs derived using different probe geometries and different analysis techniques. The Hγ excitation cross section is also

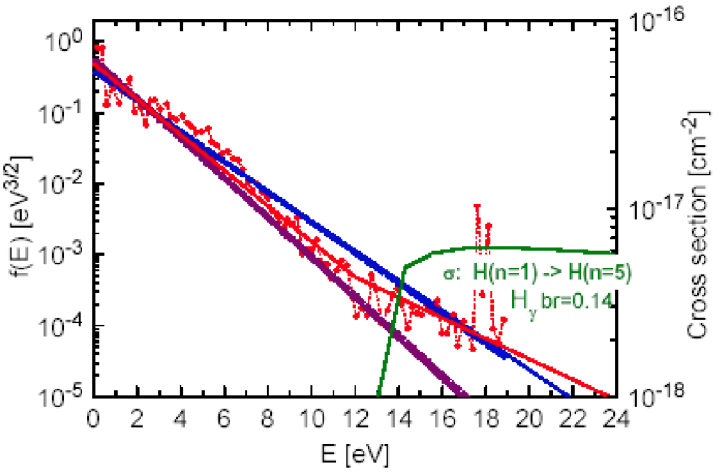


**FIGURE 13.** Normalised EEDF with fits and Hγ Excitation cross section. The red curve and points show data obtained by a spherical probe and fitted with a bi-Maxwellian EEDF the blue curve is a Maxwellian fit to the same data and the magenta curve is a Maxwellian fit to cylindrical probe data for nominally the same conditions. The green curve is the Hγ excitation cross section.

shown on the figure. The EEDF exhibits a peak at 18 eV this is as yet unexplained but is reproducible. The measurements are made in the centre of the extraction grid with source power of 45 kW and pressure of 0.3 Pa. The fits are used in a CR model that relates the measured Hγ emission to the atomic hydrogen density in the extraction region of the KAMABOKO source. The same calculation is also done based on the electron temperature as derived from the classical Langmuir-Mott Smith Theory of electron collection for Langmuir probes and the electron density as derived from the BRL method of ion collection for a cylindrical probe.

$$n_H = \frac{\varepsilon_{H\gamma}}{n_e X_{H\gamma,em}(T_e)}$$

The neutral gas density was determined from $n_0 = P/kT_{Gas}$ to be $1.1\times10^{19}$ $m^{-3}$.

Table 2 shows a summary of the results presented in the form of ratio of atomic to molecular hydrogen . The results show that only the spherical probe gives sensible output. This may due to the fact that the spherical probe is less sensitive to anisotropic electron energy distributions that are assumed to be present near the filter field. It is clear from the values of these ratios and the uncertainty of the data presented in Fig. 13 that successful and reliable interpretation of Hγ emission data is dependant on the availability of accurate fittings of the EEDF, especially in the high energy range. It is not sufficient to assume a single Maxwellian distribution for input into the CR model, it requires an expression that more faithfully represents the distribution function. In order to achieve this, the probe system requires a dynamic range covering 5 or more orders of magnitude. A new version of the system designed to achieve this is currently being tested.

**TABLE 2**. Summary of results from Hγ OES employed to determine atomic hydrogen density.

| Probe Geometry | EEDF fit | $T_e$ (eV) | $n_H/n_0$ |
|---|---|---|---|
| Spherical | Maxwellian | 2.05 | **0.43** |
| Spherical | Bi Maxwellian | $T_{e1}$ 1.73 , $T_{e2}$ 3.0 | **0.6** |
| Cylindrical | Maxwellian | 1.53 | **5.34** |
| Cylindrical | None: $T_e$ derived from Langmuir-Mott Smith Theory | 1.4 | **12.07** |

## Conclusion

Plasma parameters in the extraction region of KAMABOKO III source were determined and the EEDF was found to be non-Maxwellian with an effective electron temperature higher than the inferred Maxwellian temperature. A higher effective electron temperature, in the extraction region, has an effect on both the production and the destruction of negative ions. Firstly one would expect an increase in negative ion

destruction due to electron detachment. The higher electron temperature would also lead to a reduction in negative ion production due to dissociative attachment. The rate coefficient for $H^-$ production via the dissociative attachment channel was calculated for a Maxwellian distribution with $T_e$ =2 and real distribution of $T_{eff}$=3. It was found that the rate coefficient is a about factor of ~1.6 higher for the Maxwellian distribution. The same calculation for the rate coefficient for the process of negative ion destruction due to electron detachment shows an increase by a factor of 5 for the measured distribution compared to the fitted Maxwellian distribution. Hence, to model and optimise the production of negative ions, it is clearly necessary to know the form of the EEDF.

## ACKNOWLEDGEMENTS

This work was funded jointly by the United Kingdom Engineering and Physical Sciences Research Council and by the European Communities under the contract of Association between EURATOM and UKAEA. The views and opinions expressed herein do not necessarily reflect those of the European Commission.

## REFERENCES

1. Boyd R.L.F and Twiddy N.D., Proc.Roy.Soc **53** p250 part A 1959.
2. Trainham R., Jacquot C., Riz D., Simonin A., Miyamoto K., Fugiwara Y., and Okumura Y., Rev. Sci. Instrum. **69**, 926 1998.
3. U Fantzs *et al Nuclear Nucl. Fusion* **46** 297-306 2006.
4. Allen J.E., Boyde R.L.F. and Reynolds P., Proc.Phys.Soc.(London) **B70**, 297 (1957).
5. Laframboise J.G.Univ.Toronto Inst.Aerospace Studies Report No.100 (1966).
6. Bernstein I.B. and Rabinowitz I.N., Phys.Fluid **2**, 112 (1959).
7. Langmuir I .and Mott-Smith H. Gen.Elect.Rev. **27** ,449, 1924.
8. Godyak V.A., Piejak R.B, and Alexandrovich B, J.Appl.Phys **8**, 73 (1993).
9. Druyvesteyn, M.J. Z. Phys. 64, p790, 1930.
10. Kilvington A. I. , Jones R.P and Swift J.D. J.Sci.Instrum., **44,** 517 (1967).
11. D.Homfray and B.Crowley SOFT 2006 to be published.
12. rslankekov R.R, Khromov N.A and Kudryavtsev A.A, Plasma sources Sci. Technol. 3 528 (1994).
13. Friedland L, and Kagan Yu, J.PhysD:Appl.Phys **12,** 739 1979.
14. Magnus F.and Gudmundsson J.T, *Digital Smoothing of the Langmuir Probe I-V characteristic* Report No.RH-20-2002, Science Institute, University of Iceland (2002).
15. Janev R.K *et al. Elementary processes in Hydrogen-Helium Plasmas* Springer-Verlag, Berlin-Heidelberg, (1985).
16. Chen F.F. in *Plasma Diagnostic Techniques* (Academic Press, New York) Chapter 4 113.